Theor Chem Acc (2012) 131:1165
DOI 10.1007/s00214-012-1165-3

REGULAR ARTICLE

Relativistic coupled cluster calculations of the electronic structure of KrH^+, XeH^+ and RnH^+

Francesco Ferrante · Giampaolo Barone · Dario Duca

Received: 28 June 2011 / Accepted: 13 September 2011 / Published online: 2 March 2012

Abstract Potential energy curves of NgH^+ cations (Ng = Kr, Xe, Rn) were obtained by using four-component relativistic CCSD(T) coupled cluster calculations. Dissociation energies, equilibrium bond lengths, electronic properties, such as dipole moments and electric field gradients at the nuclei, and the related spectroscopic parameters of the electronic ground state have been determined. The results obtained for KrH^+ and XeH^+ are in good agreement with available experimental data, while those for RnH^+ have been determined for the first time at this level of theory.

Keywords Relativistic coupled cluster · protonated noble gases · spectroscopic constants

1 Introduction

The formation, stability and physical–chemical properties of noble-gas (Ng) hydrides, as neutral, cationic or anionic species, have been subjects of several experimental and theoretical studies. It is well known, for example, that the NgH^- anions (Ng = He, Ne and Ar) are weakly bound systems, characterized by quite flat potential energy curves and long equilibrium distances, due to the interaction between the negative hydride ion H^- and the polarized Ng atom [1–3]. The van der Waals NgH neutral species (Ng = He, Ne, Ar, Kr, Xe) are also defined as Rydberg molecules, [4–6] because their excited states consist of one cationic NgH^+ core related to one Rydberg electron.

The protonated NgH^+ (Ng = He, Ne, Ar, Kr and Xe) species can be experimentally produced by electron impact on noble gas + hydrogen mixtures [7, 8]. Spectroscopic studies of neutral NgH molecules (Ng = Ne, Ar, Kr and Xe) [6, 9] revealed that the cationic species, generated at high energies, are characterized by relatively deep and harmonic-shaped curves, compared to the analogous curves of the ground state of the neutral species. These compounds are also of interest from an astrophysical point of view, since recent investigations suggest that the noble gas could be trapped by H_3^+ ions to form NgH_3^+ and that NgH^+ (Ng = Ar, Kr, Xe) cations could be formed in protoplanetary disks outside the solar system, following the dissociation reaction: $NgH_3^+ \rightarrow NgH^+ + H_2$ [10].

In the latter paper, it is claimed that the sequestration of He and Ne should not occur even at temperatures down to 30 K since they form very labile NgH_3^+ complexes. However, an additional explanation could be given by considering the easiness of the proton transfer reaction $NgH^+ + H_2 \rightarrow Ng + H_3^+$. As a matter of fact, mass spectrometry measurements have shown that the amount of NgH^+ species, present in Ng/H_2 or $Ng/H_2/C_2H_4$ gas mixtures, increases with increasing atomic mass of Ng [8, 7]. This evidence can be related to the strength of the proton transfer reaction of NgH^+ that apparently decreases by increasing the atomic mass along the group [8]. Furthermore, an exothermic proton transfer reaction of NgH^+ with ethylene was evidenced [7]: $NgH^+ + C_2H_4 \rightarrow Ng + C_2H_5^+$ The conversion rate constant of the reaction above and the amount of $C_2H_5^+$ monotonously decrease by increasing the atomic number of Ng. Such trend was explained by

Dedicated to Professor Vincenzo Barone and published as part of the special collection of articles celebrating his 60th birthday.

F. Ferrante (✉) · G. Barone · D. Duca
Dipartimento di Chimica "S. Cannizzaro",
Università degli studi di Palermo, Viale delle Scienze,
Parco d'Orleans II, Palermo 90128, Italy
e-mail: francesco.ferrante@unipa.it

considering that in the ion chamber, under similar conditions, the internal energy of NgH^+ decreases by increasing the atomic mass of Ng [7]. An interesting feature of the dissociation curve of protonated noble gas is related to the observation that while for Ng = He, Ne, Ar and Kr, the dissociation curve is described by the reaction: $NgH^+ \rightarrow Ng + H^+$ [8, 11, 12], for Ng = Xe and plausibly Rn, the dissociation curve is described by the reaction: $NgH^+ \rightarrow Ng^+ + H$ [12–14].

It is worth mentioning that several accurate quantum chemical calculations of the electronic structure of Ng hydrides (Ng = He, Ne, Ar, Kr), both ionic and neutral, have been reported in the literature [15–18]. On the other hand, those involving XeH^+ and RnH^+ have been performed by using relativistic pseudopotentials in nonrelativistic approaches [19] or by the consideration of scalar relativistic effects through the zeroth-order regular approximation [20] or by the inclusion of corrective terms to take into account spin-orbit effects [21].

In the present paper, we have revisited the electronic structure and the dissociation curve of KrH^+, XeH^+ and RnH^+ employing a fully relativistic coupled cluster approach, with the aim of verifying the relativistic effects influence on the rotovibrational spectroscopic parameters in their ground electronic state. The results obtained for KrH^+ and XeH^+ have been compared to the ones available by experimental studies concerning the dissociation curves and rotational and vibrational spectroscopic parameters [22, 23]. Such benchmarking studies are essential in order to validate the approach employed for characterizing RnH^+. It is to emphasize that calculations on the latter are especially interesting because it cannot be easily investigated by experimental procedures, due to the radioactive instability of Rn and because it can be expected that relativistic contributions in the RnH^+ species must be larger than those observed in the other Group-18 elements. In this respect, calculated rotovibrational spectroscopic properties, which take into account relativistic effects in RnH^+, could be, for example, helpful for its experimental characterization. Furthermore, the relativistic results obtained for RnH^+ can be employed as a reference for studying features of the group-18 superheavy $118H^+$ species [24, 25].

2 Computational details

The four-component relativistic Dirac-Coulomb CCSD(T) approach [26, 27] has been used to calculate the electronic structure and the potential energy curves of the protonated noble gases. The fully decontracted triple zeta quality basis set provided by Dyall [28] has been used for Kr, Xe and Rn, augmented with 1s1p1d1f diffuse functions and 2f1g core correlating functions. Final basis set schemes are as follows: Kr: 24s17p11d4f1g, Xe: 29s22p16d4f1g and Rn: 31s27p18d12f1g. The uncontracted functions of aug-cc-pVTZ basis set by Dunning, 6s3p2d, have been centered on the proton. Small basis sets for relativistic calculations have been generated by kinetic balance. For computational efficiency, SS integrals have not been included in the calculations. A total of 26 electrons have been considered in the coupled cluster calculations for all NgH^+ species, being correlated 162, 204 and 212 virtual spinors for KrH^+, XeH^+ and RnH^+, respectively. The dipole moments and the electric field gradients at nuclear positions have been calculated by using the MP2 gradient. The energy of the $NgH^+ \rightarrow Ng + H^+$ dissociation has been evaluated by calculating the energy of the isolated noble-gas atom, including BSSE correction (estimated *ca.* 0.15 eV, irrespective of the noble gas). Energies of the $NgH^+ \rightarrow Ng^+(^2P_{3/2}) + H$ dissociation have conversely been obtained by considering the first ionization energy, E_I, of the involved noble-gas atom. The E_I values have been calculated at the CCSD level by using the Fock space formalism [29]. Finally, in order to estimate how relativity affects the results, the same methods and basis sets have been used to perform nonrelativistic calculations with the Lévy–Leblond Hamiltonian [30] and a point charge model for the nuclei. All calculations have been performed by using the DIRAC 0.8 program [31].

3 Results and discussion

Before starting a detailed analysis of the potential energy curves, we in the following discuss some properties calculated at the equilibrium geometry and the dissociation behavior of the three NgH^+ species.

Structural and energetic parameters of the three title compounds are reported in Table 1. The dipole moment of the three protonated noble gases was calculated at relativistic level at the equilibrium geometry. The calculated dipole moment of KrH^+, 1.969 D, is in excellent agreement with that determined experimentally, 1.967 D [32], and markedly improves the one previously estimated, 1.944 D [33], obtained by *ab initio* calculations. Considering that the calculated equilibrium distance of KrH^+ (see Sect. 3.1) is slighter underestimated compared to the corresponding experimental value, the explanation for such good agreement between calculated and experimental dipole moments is not straightforward. This result has in fact to be considered cautiously, taking into account the intrinsic difficulties present in the experimental determination of dipole moments of charged species [34].

Table 1 Equilibrium distance (Å), dipole moment (D), electric field gradient on the Ng nucleus (a.u.), dissociation energy (eV), ionization energy of Ng (eV) and spin-orbit splitting (SOS) in Ng^+ (eV), obtained for the three protonated noble gases KrH^+, XeH^+ and RnH^+ at relativistic (*R*) and nonrelativistic (NR) coupled cluster level

	KrH^+			XeH^+			RnH^+	
	R	NR	Exp	*R*	NR	Exp	*R*	NR
r_e	1.414	1.415	1.421[a]	1.598	1.601	1.603[f]	1.710	1.700
μ	1.969	–	1.967[b]	1.512	–	–	1.025	–
q	8.8838	–	–	13.3819	–	–	28.0594	–
$D_e(Ng + H^+)$	4.58	4.58	4.51[c]	5.28	5.30	–	5.68	5.64
$D_e(Ng^+ + H)$[j]	4.79	5.03	–	3.64	4.09	3.81[g]	2.64	3.68
E_I	13.81	14.06	14.00[d]	11.96	12.40	12.13[h]	10.56	9.07
SOS	0.67	–	0.65[e]	1.31	–	1.312[i]	3.81	–

[a] Ref. [22], [b] Ref. [32], [c] Ref. [12], [d] Ref. [38, 39], [e] Ref. [40], [f] Ref. [13], [g] Ref. [14], [h] Ref. [41, 42], [i] Ref. [42], [j] $^2P_{3/2}$ state in the relativistic case

To our knowledge, the experimental value of the dipole moment of XeH^+ has not been reported in the literature. The value obtained in the present paper, 1.512 D, is smaller than that already calculated, 1.551 D, by Klein and Rosmus [35].

From Table 1, it is evident that for KrH^+ the dissociation energy to $Kr + H^+$ is lower than that leading to $Kr^+ + H$, both at relativistic and nonrelativistic levels. Hence, relativity seems to have no sensible effect, being the relativistic and nonrelativistic results equal, 4.58 eV, and within 1.5% from the experimental D_e value of 4.51 eV [8, 11, 12]. The relativistic effect is indeed very small also for the dissociation energy values to $Ng + H^+$ calculated for XeH^+ and RnH^+, because there is no spin-orbit coupling in these cases. The dissociation energy of XeH^+ experimentally determined, which produces $^2S_{1/2}$ H and $^2P_{3/2}Xe^+$, is equal to 3.81 eV [12–14]. The D_e value calculated at relativistic level for XeH^+, 3.64 eV, is lower of about 4.5% than the corresponding experimental value and is in worst agreement than the value previously calculated by Peterson and co-workers [19]. However, in the latter paper, the dissociation energy to $^2S_{1/2}$ H and $^2P_{3/2}Xe^+$ has been determined by using the experimental value of the ionization energy of Xe, in the following equation: $D_e(^2P_{3/2}Xe^+ + {}^2S_{1/2}) = D_e(Xe + H^+) + E_I(Xe) - E_I(H)$, where the value of 13.61 eV has been used for $E_I(H)$. Since the calculated E_I of Xe to $^2P_{3/2}Xe^+$, 11.96 eV, is lower of 0.17 eV than the experimental value, such error is propagated in the D_e value. If we use the E_I experimental value of Xe, we obtain 3.80 eV in perfect agreement with the experiment. As a matter of fact, while the ionization energy of Xe to $^2P_{3/2}Xe^+$ is strongly affected by spin-orbit coupling, the dissociation energy of XeH^+ to Xe and H^+ is not. Hence, the value of D_e that we have obtained, 3.64 eV, allows one to estimate the accuracy with which the effects of the spin-orbit coupling can be determined by relativistic *ab initio* calculations. Incidentally, the nonrelativistic calculation overestimates the experimental Xe E_I value of 0.27 eV. At the same time, the ionization energy of atomic radon is evaluated with an error of 0.19 eV with respect to the early experimental value of 10.748 eV reported by Rasmussen [36]. It is worth to note that, although the calculated effect of spin-orbit coupling is not extremely accurate on the ionization energy (which has been here evaluated without the inclusion of the perturbative correction for triple excitations), the $^2P_{3/2}$–$^2P_{1/2}$ spin-orbit splittings (SOS) in Kr^+ and Xe^+ have been determined with an excellent agreement with the experimental values (see Table 1). Interestingly, spin-orbit coupling is so large in RnH^+ that there is an inversion of the dissociation energy of $D_e(^2P_{1/2}\ Rn^+ + {}^2S_{1/2}H)$ with that of $D_e(Rn + H^+)$ and the order of the three possible dissociation energy values becomes: $D_e(^2P_{3/2}Rn^+ + {}^2S_{1/2}H) < D_e(Rn + H^+) < D_e(^2P_{1/2}Rn^+ + {}^2S_{1/2}H)$. On the other hand, for XeH^+, the order is the following: $D_e(^2P_{3/2}\ Xe^+ + {}^2S_{1/2}H) < D_e(^2P_{1/2}Xe^+ + {}^2S_{1/2}H) < D_e(Xe + H^+)$. The values of $D_e(^2P_{1/2}Ng^+)$ can be calculated by using the spin-orbit splitting data for the Ng^+ cation reported in Table 1.

The electric field gradient at the nucleus, q, is a useful parameter to determine the nuclear quadrupole moment (Q) once knowing the quadrupole coupling constant (eQq), for example, from the rotational line splitting. In particular, the calculated electric field gradient can be of particular importance for evaluating the quadrupole moment of a given radon isotope in RnH^+ from the registration of its spectrum. The fully relativistic treatment used in the present approach, together with the use of specifically tailored relativistic basis sets, allows us to think that the electric field gradients q reported in Table 1 are highly accurate. By using the nuclear quadrupole coupling constants for $^{83}KrD^+$ (549.1 MHz [11]) and $^{131}XeH^+$ (−369.5 MHz [14]), we obtain the following updated

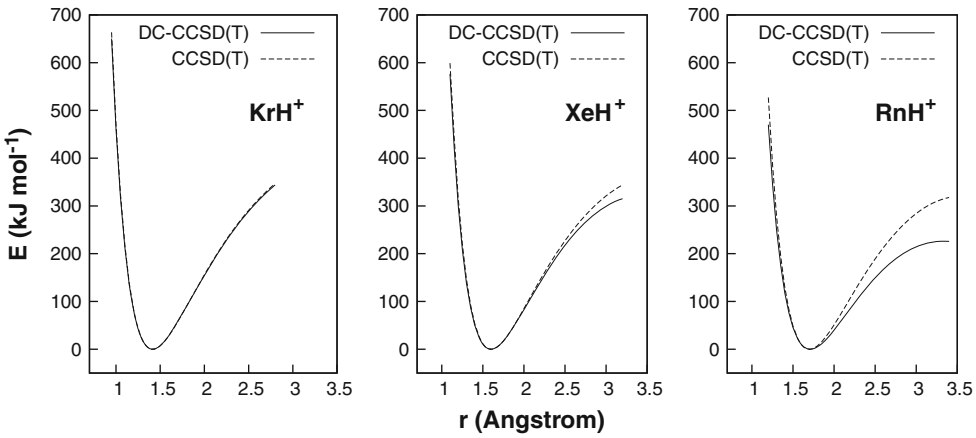

Fig. 1 The relativistic and nonrelativistic energy curves in the range $0.7r_e$–$2.0r_e$ for KrH^+, XeH^+ and RnH^+

values of nuclear quadrupole moments Q: +263.1 and −117.5 mbarn for ^{83}Kr and ^{131}Xe, respectively. Previous values of Q, +259 and −114 mbarn, were reported in the literature [37]. There is no experimental quadrupole coupling constant for RnH^+ or RnD^+. In this case, by using the nuclear quadrupole moments of ^{209}Rn reported in [37], Q = +311 mbarn, and the corresponding value of q in Table 1, we obtained the remarkably large value of eQq = 2.050 GHz for $^{209}Rn^+$.

3.1 Analysis of the potential energy curves

A Dunham analysis of the potential energy curves was performed in the bond length range $0.7r_e$–$2.0r_e$, being r_e the calculated NgH^+ equilibrium distance corresponding to the fundamental state. The potential energy curves have been obtained by a scan of the energy as a function of the internuclear distance, in steps of 0.05 Å. Near the energy minimum, the steps were reduced at 0.01 Å and in the harmonic region at 0.001 Å, for a total of about 110 points. The equilibrium distance was estimated from the analysis of the harmonic portion and was used as fixed parameter in the fitting procedure with the Dunham potential.

The analysis of the electronic structure along the dissociation curve of both XeH^+ and RnH^+ induces to think that the intersection between the (Ng + H^+) and the ($^2P_{3/2}Ng^+$ + H) potential energy curves occurs in the internuclear distance range 2.75–2.80 Å and 2.70–2.75 Å for Ng = Xe and Rn, respectively. According to the analysis of the spectroscopic constants determined in the present work (see below), the curve intersection should occur near the 11th and 8th vibration level of XeH^+ and RnH^+, respectively. The effect of the spin-orbit coupling is clear from the inspection of the dissociation curves obtained by relativistic and nonrelativistic calculations, as illustrated in Fig. 1. The latter shows that the difference between the two curves is negligible for KrH^+ and only a small effect on the values of the spectroscopic constants can be predicted, excepting the high-order ones (see Table 2). For XeH^+, a stabilization of the relativistic ($^2P_{3/2}Xe^+$ + H) compared to the nonrelativistic ($^2PXe^+$ + H) curve occurs at high r values. Such stabilization produces small curve shape variations also at internuclear distance values near the energy minimum. The effect is markedly more pronounced for RnH^+, because the spin-orbit coupling is by far larger. Such differences in the shapes of the dissociation curves of XeH^+ and RnH^+ lead to different values of the spectroscopic constants evaluated by including or not relativity in our calculations (see Tables 3 and 4).

Table 2 Dunham coefficients at relativistic (R) and nonrelativistic (NR) level for $^{84}KrH^+$ and their spectroscopic identification (SC)

	R	NR	Exp	SC
Y_{10}	2,551.1	2,567.1	2,494.7[a]	ω_e
Y_{20}	45.8	47.1	48.5[a]	$-\omega_e x_e$
Y_{30}	0.207	0.321		$\omega_e y_e$
Y_{40}	−0.017	−0.014		$\omega_e z_e$
Y_{01}	8.466	8.454	8.381[a]	B_e
Y_{11}	0.277	0.279	0.267[a]	$-\alpha_e$
$Y_{21} \times 10^3$	1.71	1.86		γ_e
$Y_{31} \times 10^4$	4.22	5.10		
$Y_{02} \times 10^4$	3.73	3.67		$-D_e$
$Y_{12} \times 10^6$	7.75	6.94		β_e
$Y_{22} \times 10^7$	−3.76	−1.86		
$Y_{03} \times 10^9$	6.74	6.11		H_e
$Y_{13} \times 10^{10}$	−2.01	−0.66		
$Y_{04} \times 10^{13}$	−3.02	−3.02		
B_0	8.328	8.315	8.248[b]	
$-D_0 \times 10^4$	3.69	3.63	3.76[b]	
$H_0 \times 10^9$	6.64	6.07	6.92[b]	

Dunham fit was performed in the range 0.95–2.80 Å. All values are in cm^{-1}

[a] Ref. [8], [b] Ref. [22]

Table 3 Dunham coefficients at relativistic (R) and nonrelativistic (NR) level for $^{132}XeH^+$ and their spectroscopic identification (SC)

	R	NR	Exp	SC
Y_{10}	2,286.6	2,320.3	2,270.0[a]	ω_e
Y_{20}	36.6	34.7	41.3[a]	$-\omega_e x_e$
Y_{30}	0.065	0.021		$\omega_e y_e$
Y_{40}	−0.021	−0.023		$\omega_e z_e$
Y_{01}	6.600	6.575	6.561[a]	B_e
Y_{11}	0.188	0.180	0.187[a]	$-\alpha_e$
$Y_{21} \times 10^3$	0.96	1.01		γ_e
$Y_{31} \times 10^4$	1.57	0.84		
$Y_{02} \times 10^4$	2.20	2.11		$-D_e$
$Y_{12} \times 10^6$	4.18	4.76		β_e
$Y_{22} \times 10^7$	−2.79	−3.77		
$Y_{03} \times 10^9$	2.94	2.90		H_e
$Y_{13} \times 10^{10}$	−1.17	−1.65		
$Y_{04} \times 10^{14}$	9.36	−6.39		
B_0	6.507	6.485	6.467[b]	
$-D_0 \times 10^4$	2.18	2.09	2.18[b]	
$H_0 \times 10^9$	2.89	2.82	2.57[b]	

Dunham fit was performed in the range 1.10–3.20 Å. All values are in cm^{-1}

[a] Ref. [12], [b] Ref. [23]

Table 4 Dunham coefficients at relativistic (R) and nonrelativistic (NR) level for $^{222}RnH^+$ and their spectroscopic identification (SC)

	R	NR	SC
Y_{10}	2,016.3	2,212.5	ω_e
Y_{20}	34.3	33.7	$-\omega_e x_e$
Y_{30}	−0.056	0.054	$\omega_e y_e$
Y_{40}	−0.031	−0.019	$\omega_e z_e$
Y_{01}	5.746	5.814	B_e
Y_{11}	0.172	0.155	$-\alpha_e$
$Y_{21} \times 10^4$	5.64	8.53	γ_e
$Y_{31} \times 10^4$	1.28	1.21	
$Y_{02} \times 10^4$	1.87	1.61	$-D_e$
$Y_{12} \times 10^6$	3.20	2.81	β_e
$Y_{22} \times 10^7$	−3.89	−1.82	
$Y_{03} \times 10^9$	1.81	1.51	H_e
$Y_{13} \times 10^{10}$	1.76	−0.57	
$Y_{04} \times 10^{14}$	−6.86	−4.02	
B_0	5.660	5.737	
$-D_0$	1.85	1.59	
H_0	1.72	1.50	

Dunham fit was performed in the range 1.20–3.20 Å. All values are in cm^{-1}

The a_i coefficients of the Dunham potential:

$$V(\xi) = a_0\xi^2\left(1 + \sum_{i=1}^{6} a_i\xi^i\right) \quad \xi = \frac{r - r_e}{r_e} \tag{1}$$

have been obtained by the fit of the calculated potential energy curves. These have been used to determine the Dunham Y_{kj} coefficients [43], which are correlated to the position of the rotovibrational spectroscopic lines by the following equation:

$$E_{v,J} = \sum_{j=1}^{4}\sum_{k=0}^{5} \rho^{2j+k} Y_{kj}\left(v + \frac{1}{2}\right)^k [J(J+1)]^j \tag{2}$$

The factors $\rho = \mu/\mu_{iso}$ can be used to evaluate the isotopic effects on the spectroscopic constants, when considering species with different reduced mass μ_{iso} compared to that of the isotope used in the calculation. This consideration can be important for Xe, which consists of five principal isotopes, three of which with abundances larger than 20% and two with abundances about 10%. The values reported in Tables 2, 3 and 4 are referred to the molecular species having the following isotopic composition: $^{84}Kr^1H^+$, $^{132}Xe^1H^+$ and $^{222}Rn^1H^+$.

The rotational spectra of $^{84}KrH^+$ and $^{86}KrH^+$ are reported in [22], with a claimed accuracy of 40 kHz in the transition frequencies. The equilibrium distance of KrH^+ calculated at both relativistic and nonrelativistic levels is smaller than that obtained experimentally of 0.007 and 0.006 Å, respectively. An analogous but slighter difference was also observed for XeH^+. The underestimation of the calculated equilibrium bond length has a direct consequence on the rotational constants B_e and B_0, which are both about 1% larger than the corresponding experimental values. This occurs because the rotovibrational coupling constant α_e only marginally affects the ground vibrational state rotational constant B_0. The calculated values of the fourth- and sixth-order centrifugal distortion constants for the ground vibrational state, D_0 and H_0, are both smaller of 2 and 4% than the corresponding experimental values, respectively. Remarkably, such errors are about three times larger in the corresponding nonrelativistic case. The relativistic correction to the fundamental frequency, ω_e, is of only 16 cm^{-1}, and the experimental value is overestimated by about 2 and 3% at relativistic and nonrelativistic levels, respectively. The calculated first anharmonicity constant, $\omega_e x_e$, on the other hand, underestimates the experimental value of about 6 and 3% at relativistic and nonrelativistic levels, respectively. The agreement between calculated and experimental values of the spectroscopic parameters is worst than that obtained by Peterson et al. [19], likely because the equilibrium distance calculated in the latter paper is slightly larger than that obtained in the present work. However, it is interesting to note that in the paper by Peterson et al., the equilibrium bond lengths calculated at the CCSD(T)/aug-cc-pv5Z-PP level for all the diatomics

there reported are systematically overestimated, of 0.005–0.011 Å, with respect to the corresponding experimental values. The only exception is KrH^+, for which experimental and calculated bond lengths agree within 0.001 Å. These findings, in our opinion, suggest the need of confirming the experimental result on the Kr–H distance in KrH^+.

A pure rotational spectrum of XeH+, with an estimated accuracy of 35 kHz on the transition frequencies, is reported by Ohtaki et al. [23], for all known isotopes and for both hydrogenated and deuterated species. Also in this case, the equilibrium bond distance is underestimated of 0.3%, with consequent overestimates of 0.6% on B_e and B_0. In comparison with KrH^+, however, the α_e and D_0 constants are more accurately determined, with an error of less than 0.5%. The calculated H_0 constant, on the other hand, is larger of about 12% than the corresponding experimental value. For XeH^+, the bond distance calculated at nonrelativistic level is in better agreement with the experimental value, and consequently the same occurs also for B_e and B_0. However, other constants show a larger deviation than that obtained at relativistic level, for example, $\alpha_e = -4\%$, $D_0 = -4\%$, $H_0 = -14\%$.

A slight deformation of the calculated potential energy curve, for example, due to spin-orbit coupling, could affect the relativistic fundamental vibration frequency that is 16 cm^{-1} (0.7%) and 50 cm^{-1} (2.2%) higher than the experimental value at relativistic and nonrelativistic levels, respectively. The relativistic fundamental vibration frequency of XeH^+ is comparable to that obtained by Runeberg et al. [21] by nonrelativistic CCSD(T) calculations, with corrections for the BSSE and spin-orbit coupling. On the other hand, the first anharmonicity constant is underestimated by 11 and 16% at relativistic and nonrelativistic level, respectively.

To the best of our knowledge, no experimental data have been reported in the literature concerning the structure and spectroscopic constants of RnH^+. The only available data are relative to CCSD(T) calculations with relativistic pseudopotential basis sets [19] and DFT calculations with scalar relativistic contributions evaluated by the ZORA approximation [20]. Being our calculations fully relativistic, the difference between the relativistic equilibrium distance evaluated in the present work and that previously obtained should be mainly attributable to the deformation of the potential energy curve due to the occurrence of a strong spin-orbit coupling at large internuclear distance, where the ($^2P_{3/2}Rn^+ + H$) character must be taken into account. Such curve deformation causes a lowering of the fundamental vibration frequency and a slight increase in the relativistic equilibrium distance compared to the nonrelativistic one. In fact, while the nonrelativistic equilibrium distance of RnH^+, 1.700 Å, is in good agreement with those previously calculated, 1.6957 Å [19] and 1.702 Å [20], the relativistic value is slightly larger, 1.710 Å. Analogously, the nonrelativistic vibration frequency is higher of about 200 cm^{-1} than the corresponding relativistic value (see Table 4) and of about 140 cm^{-1} compared to the result reported in Peterson et al. [19]. Of course, the consistent difference in the shape of the relativistic and nonrelativistic potential energy curves of RnH^+ produces large effects on the centrifugal and rotovibrational coupling constants, which show large percentage changes and also two sign variations. Considering that for XeH^+ the relativistic treatment leads to a by far better agreement with the experimental fundamental frequency, and considering also that relativistic effects increase with the atomic number, in our opinion the relativistic results obtained for the protonated radon are more reliable than those obtained at nonrelativistic level.

In Tables 2, 3 and 4, the high-order spectroscopic constants are also reported. They have not been discussed since neither experimental nor calculated corresponding data are reported in the literature. Such constants are so tiny that their values are strongly affected by the fit procedure. Indeed, they are only rarely used in the interpretation of biatomic molecule spectra.

4 Conclusions

In this work, the potential energy curves and the spectroscopic parameters of the protonated forms of the three heavier noble gases, KrH^+, XeH^+ and RnH^+, have been obtained by fully relativistic coupled cluster calculations. The relativistic contributions have been assessed by comparison with the values calculated at the same nonrelativistic level of theory. The obtained results are in good agreement with the available experimental data, though the calculations slightly underestimate the bond length in KrH^+ and, to a lesser extent, in XeH^+. A small change in the shape of the XeH^+ potential energy curve, due to the intersection of the ($Xe + H^+$) with the ($^2P_{3/2}Xe^+ + H$) curve at higher internuclear distances, improves the agreement with the experimental vibrational and rotovibrational constants with respect to the nonrelativistic results. The potential energy curve deformation is particularly evident for RnH^+, whose structural, electronic and spectroscopic properties are here reported for the first time at fully relativistic level. These data could be used for the experimental characterization of RnH^+, which is made difficult by the radon low abundance and high radioactive instability.

Acknowledgments We thank the "Fondazione Banco di Sicilia" for the financial support supplied to assemble the "Iride" computer cluster (convenzione PR13.b/07).

References

1. Li Y, Lin CD (1999) Phys Rev A 60:2009–2014
2. Robicheaux F (1999) Phys Rev A 60:1706–1709
3. Vallet V, Bendazzoli GL, Evangelisti S (2001) Chem Phys 263:33–40
4. Braga JP, Murrella JN (1984) Mol Phys 53:295–299
5. Douay M, Rogers SA, Bernath PF (1988) Mol Phys 64:425–436
6. Lo JMH, Klobukowski M, Bielinska-Waz D, Diercksen GHF, Schreiner EWS (2005) J Phys B: At Mol Opt Phys 38:1143–1159
7. Smith RD, Futrell JH (1976) Int J Mass Spect Ion Phys 20:71–76
8. Johns JWC (1984) J Mol Spectr 106:124–133
9. Moller T, Beland M, Zimmerer G (1987) Chem Phys Lett 136:551–556
10. Mousis O, Pauzat F, Ellinger Y, Ceccarelli C (2008) Astrophys J 673:637–646
11. Warner HE, Conner WT, Woods RC (1984) J Chem Phys 81:5413–5416
12. Hunter EP, Lias SG (1998) J Phys Chem Ref Data 27:413–656
13. Rogers SA, Brazier CR, Bernath PF (1987) J Chem Phys 87:159–162
14. Peterson KA, Petrmichl RH, Wood RC (1991) J Chem Phys 95:2352–2360
15. Liu DJ, Ho WC, Oka T (1987) J Chem Phys 87:2442–2446
16. Partridge H, Schwenke DW, Bauschlicher CW (1993) J Chem Phys 99:9776–9783
17. Schutte CJH (2002) Chem Phys Lett 353:389–395
18. Sebera CJ, Spirko V, Fiser J, Kraemer WP, Kawaguchi K (2004) J Mol Struct 695(696):5–11
19. Peterson KA, Figgen D, Goll E, Stoll H, Dolg M (2003) J Chem Phys 119:11113–11123
20. Pierrefixe SCAH, Poater J, Im C, Bickelhaupt FM (2008) Chem Eur J 14:6901–6911
21. Runeberg N, Seth M, Pyykkö P (1995) Chem Phys Lett 246:239–244
22. Linnartz H, Zink LR, Evenson KM (1997) J Mol Spectr 184:56–59
23. Ohtaki Y, Matsushima F, Odashima H, Takagi K (2001) J Mol Spectr 210:271–274
24. Nash CS (2005) J Phys Chem A 109:3493–3500
25. Pershina V (2009) Russ Chem Rev 78:1153–1171
26. Visscher L, Lee TJ, Dyall KG (1996) J Chem Phys 105:8769–8776
27. Pernpointner M, Visscher L (2003) J Comp Chem 24:754–759
28. Dyall KG (2002) Theor Chem Acc 108:335–340; erratum (2003) Theor Chem Acc 109:284; revision (2006) Theor Chem Acc 115:441. Basis sets available from the Dirac web site, http://dirac.chem.sdu.dk
29. Visscher L, Eliav E, Kaldor U (2001) J Chem Phys 115:9720–9726
30. Lévy-Leblond JM (1967) Commun Math Phys 6:286–311
31. DIRAC, a relativistic ab initio electronic structure program, Release DIRAC08 (2008), written by Visscher L, Jensen HJAa, Saue T, with new contributions from Bast R, Dubillard S, Dyall KG, Ekström U, Eliav E, Fleig T, Gomes ASP, Helgaker TU, Henriksson J, Ilias M, Jacob ChR, Knecht S, Norman P, Olsen J, Pernpointner M, Ruud K, Salek P, Sikkema J (see http://dirac.chem.sdu.dk)
32. Molski M (2002) Mol Phys 100:3545–3552
33. Rosmus P, Reinsch EA (1980) Z Naturforsch A 35:1066–1070
34. Linnartz H, Havenith M, Zwart E, Meerts WL, Ter Meulen JJ (1992) J Mol Spectr 153:710–717
35. Klein R, Rosmus P (1984) Z Naturforsch A 39:349–353
36. Rasmussen E (1933) Z Phys 80:726–734
37. Pyykkö P (2008) Mol Phys 106:1965–1974
38. Yoon S, Glab WL (1994) J Phys B: At Mol Opt Phys 27:1433–1441
39. Brandi F, Hogervorst W, Ubachs W (2002) J Phys B At Mol Opt Phys 35:1071–1084
40. Kaufman V (1993) J Res Natl Inst Stand Tech 98:717–724
41. Knight DL, Wang L (1985) J Opt Soc Am B 2:1084–1087
42. Brandi F, Velchev I, Horgervorst W, Ubachs W (2001) Phys Rev A 64:032505
43. Dunham JL (1932) Phys Rev 41:721–731